Asian Journal of Chemistry; Vol. 28, No. 5 (2016), 1108-1114

ASIAN JOURNAL OF CHEMISTRY

http://dx.doi.org/10.14233/ajchem.2016.19601

Effects on Photocatalytic Degradation and Hydrogen Evolution of TiO_2 Coated $CaLa_2(MoO_4)_4$ and $CaLa_2(MoO_4)_4$:Er/Yb Nano Core-Shells and their Upconversion Photoluminescence

WON-CHUN OH, SHE YE, JUNG GYU PARK and CHANG SUNG LIM*

Department of Advanced Materials Science & Engineering, Hanseo University, Seosan 356-706, Republic of Korea

*Corresponding author: Tel/Fax: +82 41 6601445; E-mail: cslim@hanseo.ac.kr

Received: 7 September 2015; *Accepted*: 3 October 2015; *Published online*: 30 January 2016; AJC-17756

Titanium(IV) dioxide coated $CaLa_2(MoO_4)_4$ and $CaLa_2(MoO_4)_4$:Er/Yb nano core-shells were successfully synthesized using two-step procedures of the microwave sol-gel and ultrasonic methods. Well-crystallized nano core- shells showed a fine and homogeneous morphology with particle sizes of 10-20 nm. The degradation efficiency for TiO_2 coated $CaLa_2(MoO_4)_4$ and $CaLa_{1.7}(MoO_4)_4$:$Er_{0.1}Yb_{0.2}$ nano core-shells under visible light resulted in the order as 10 wt % > 15 wt % > 5 wt %. Quantum yield of the nano core-shells for the hydrogen evolution provided the best result for 10 wt % of TiO_2 coated $CaLa_{1.5}(MoO_4)_4$:$Er_{0.05}Yb_{0.45}$ with 6.19 %, using Na_2S/Na_2SO_3 as the reagent. Under excitation at 980 nm, the upconversion of $CaLa_{1.7}(MoO_4)_4$:$Er_{0.1}Yb_{0.2}$ and $CaLa_{1.5}(MoO_4)_4$:$Er_{0.05}Yb_{0.45}$ particles exhibited a strong 525 nm and a weak 550 nm emission bands in the green region. The Commission Internationale de L'Eclairage (CIE) diagram showed a good match with yellowish green emissions.

Keywords: Photocatalytic degradation, Hydrogen evolution, Nano core-shells, Upconversion photoluminescence.

INTRODUCTION

Photocatalysts of TiO_2 is the most widely used semiconductor in control of environmental pollution, energy storage and conversion, various sensors and photovoltaic batteries, due to its unique photo-electric properties, high chemical stability, low cost and safety for human and the environmental applications [1-3]. The optimization and improvement of TiO_2 as a photocatalyst are required for technical applications of hybrid photocatalysis in the future [4-6]. Upconversion (UC) process induced by the trivalent lanthanide doped photoluminescence converts long-wavelength excitation radiation in the infrared or near infrared region to higher energy emission radiation from ultraviolet to infrared. These upconversion photoluminescence particles have potential applications in various fields, including biomedical imaging, owing to their unique upconversion characteristics to overcome many of the current limitations for future photoluminescence materials [7-9].

Application of upconversion particles as a energy-modifier may be effective to employ the NIR light for TiO_2 photocatalyst, because upconversion particles can efficiently upconvert the NIR light into UV emission [10-13]. Precise combination of upconversion particles and TiO_2 can produce a new type of hybrid photocatalysts to play an important role under both the UV and NIR irradiation, improving the utilization range of solar energy. Quantum efficiency of the upconversion particles can be improved surface coating of a crystalline core-shell [14-16]. The coated crystallines of upconversion particles reduces defects on the surface and minimizes quenching of the excited states of lanthanide ions. In order to reduce these defects, the growth of crystalline core-shell of a suitable substance around each nano crystals to form the core-shell structures should be considered as an effective coating to improve luminescence efficiency [17-19]. Hydrogen energy is considered as the most important form of clean and storable energy [20-22]. Therefore, uniform TiO_2 coated upconversion luminescence core-shells with desirable morphology and photocatalytic activity as well as hydrogen evolution are required for their future applications.

In this study, TiO_2 coated undoped $CaLa_2(MoO_4)_4$ and doped $CaLa_2(MoO_4)_4$:Er^{3+}/Yb^{3+} nano core-shells were synthesized by two-step procedures using the microwave sol-gel and ultrasonic methods. $CaLa_{2-x}(MoO_4)_4$:Er^{3+}/Yb^{3+} phosphors with doping concentrations of Er^{3+} and Yb^{3+} (x = for Er^{3+} + Yb^{3+}, Er^{3+} = 0.05, 0.1, 0.2, respectively and Yb^{3+} = 0.2, 0.45) phosphors were prepared *via* the microwave sol-gel route. Subsequently, the TiO_2 coated $CaLa_2(MoO_4)_4$ and $CaLa_2(MoO_4)_4$:Er^{3+}/Yb^{3+} particles were synthesized using a single ultrasonic method under solid state. The catalytic efficiency of the hybrid material composites was evaluated by photo degradation of methylene blue dye and hydrogen evolution under visible light. The synthesized particles were characterized by X-ray diffraction

(XRD) and transmission electron microscopy (TEM). The optical pro-perties were examined comparatively using photoluminescence emission and Commission Internationale de L'Eclairage (CIE) chromaticity.

EXPERIMENTAL

Preparation of $CaLa_2(MoO_4)_4$ and $CaLa_{2-x}(MoO_4)_4$ phosphors: For the preparation of $CaLa_2(MoO_4)_4$, $CaLa_{1.8}(MoO_4)_4$:$Er_{0.2}$, $CaLa_{1.7}(MoO_4)_4$:$Er_{0.1}Yb_{0.2}$ and $CaLa_{1.5}(MoO_4)_4$:$Er_{0.05}Yb_{0.45}$ compounds with doping concentrations of Er^{3+} and Yb^{3+} (Er^{3+} = 0.05, 0.1, 0.2 and Yb^{3+} = 0.2, 0.45), available amounts of $Ca(NO_3)_2{\cdot}4H_2O$ (99 %, Sigma-Aldrich, USA), $La(NO_3)_3{\cdot}6H_2O$ (99 %, Sigma-Aldrich, USA), $(NH_4)_6Mo_7O_{24}{\cdot}4H_2O$ (99 %, Alfa Aesar, USA), $Er(NO_3)_3{\cdot}5H_2O$ (99.9 %, Sigma-Aldrich, USA), $Yb(NO_3)_3{\cdot}5H_2O$ (99.9 %, Sigma-Aldrich, USA), citric acid (99.5 %, Daejung Chemicals, Korea), NH_4OH (A.R.), ethylene glycol (A.R.) and distilled water were used. To prepare $CaLa_2(MoO_4)_4$, 0.4 mol % $Ca(NO_3)_2{\cdot}4H_2O$ and 0.4 mol % $(NH_4)_6Mo_7O_{24}{\cdot}4H_2O$ were dissolved in 20 mL of ethylene glycol and 80 mL of 5 M NH_4OH under vigorous stirring and heating. Subsequently, 0.8 mol % $La(NO_3)_3{\cdot}6H_2O$ and citric acid were dissolved in 100 mL of distilled water under vigorous stirring and heating. The molar ratio of citric acid to total metal ions was 2:1. Then, the solutions were mixed together under vigorous stirring and heating at 80-100 °C. At the end, highly transparent solutions were obtained and adjusted to pH=7-8 by the addition of NH_4OH or citric acid. In order to prepare $CaLa_{1.8}(MoO_4)_4$:$Er_{0.2}$, the mixture of 0.72 mol % $La(NO_3)_3{\cdot}6H_2O$ with 0.08 mol % $Er(NO_3)_3{\cdot}5H_2O$ was used for the creation of the rare earth solution. In order to prepare $CaLa_{1.7}(MoO_4)_4$:$Er_{0.1}Yb_{0.2}$, the mixture of 0.68 mol % $La(NO_3)_3{\cdot}6H_2O$ with 0.04 mol % $Er(NO_3)_3{\cdot}5H_2O$ and 0.08 mol % $Yb(NO_3)_3{\cdot}5H_2O$ was used for the rare earth solution. In order to prepare $CaLa_{1.5}(MoO_4)_4$:$Er_{0.05}Yb_{0.45}$, the rare earth containing solution was generated using 0.6 mol % $La(NO_3)_3{\cdot}6H_2O$ with 0.02 mol % $Er(NO_3)_3{\cdot}5H_2O$ and 0.18 mol % $Yb(NO_3)_3{\cdot}5H_2O$. The transparent solutions were employed into a microwave oven operating at a frequency of 2.45 GHz with a output-power of 1250 W for 30 min. Finally, the light yellowish transparent sols were dried at 120 °C in a dry oven to obtain black dried gels. The dried gels were ground and annealed at 900 °C for 16 h with 100 °C intervals between 600-900 °C. Finally, white particles were obtained for $CaLa_2(MoO_4)_4$ and pink particles for doped compositions.

Preparation of TiO_2 coated $CaLa_2(MoO_4)_4$ and $CaLa_{2-x}(MoO_4)_4$:Er/Yb: The obtained undoped $CaLa_2(MoO_4)_4$ and doped $CaLa_{2-x}(MoO_4)_4$:Er/Yb were further decorated with TiO_2 nanoparticles by the ultrasonic method. 2 mL of TNB (about 6.5×10^{-5} mol) was used to add in 10 mL ethanol solution, followed by magnetic stirring for 5 min. 10 mL distilled water was added dropwise into the solution with constant stirring. Then as-prepared $CaLa_2(MoO_4)_4$ and $CaLa_{2-x}(MoO_4)_4$:Er/Yb of 0.1 g, 0.2 g and 0.3 g were added with 30 mL ethylene glycol into the solution, respectively. The solutions were constantly stirred and ultra-sonicated with a power of 750 W using Ultrasonic Processor (VCX 750, Korea) for 4 h. After completion, the black solution was filtered and washed 3 times with deionized water and ethanol. The obtained samples were dried at 120 °C. Finally, the samples were heated at 600 °C for 1h. The weight ratios of $CaLa_2(MoO_4)_4$ and $CaLa_{2-x}(MoO_4)_4$:Er/Yb to TNB were approximately 5 %, 10 %, 15 %, respectively.

Characterization of phase identification, upconversion properties, photocatalytic activity and hydrogen evolution: The phase compositions of the synthesized nano core shells of TiO_2 coated $CaLa_2(MoO_4)_4$, $CaLa_{1.8}(MoO_4)_4$:$Er_{0.2}$, $CaLa_{1.7}(MoO_4)_4$:$Er_{0.1}Yb_{0.2}$ and $CaLa_{1.5}(MoO_4)_4$:$Er_{0.05}Yb_{0.45}$ were identified using XRD (D/MAX 2200, Rigaku, Japan). The microstructure and surface morphology of the nano core shells were observed using TEM (JEM-2010, JEOL, Japan). The photoluminescence spectra of the $CaLa_2(MoO_4)_4$ and doped $CaLa_{2-x}(MoO_4)_4$:Er/Yb were recorded using a spectrophotometer (Perkin Elmer LS55, UK) at room temperature. The colour coordinates of the phosphors were evaluated by the CIE chromaticity diagram.

Photocatalytic activities of the samples were evaluated by the degradation of methylene blue solution under irradiation of visible light (8 W, Fawoo, Lumidas-H, Korea, $\lambda = 420$ nm). In an ordinary photocatalytic test performed at room temperature, 0.05 g photocatalyst was added to 50 mL of 2.0×10^{-5} mol/L methylene blue solution [23], which was hereafter considered as the initial concentration (c_0). The mixture was sonicated for 10 min and stirred for 120 min in the dark in order to reach adsorption–desorption equilibrium. The first sample was taken out just before the light was turned on in order to determine the dye concentration in solution after dark adsorption, which was henceforth considered as the initial concentration (c_{ads}). Samples were then withdrawn regularly from the reactor by an order of 30, 60, 90 and 120 min, immediately centrifuged to separate any suspended solid. The clean transparent solution was analyzed by using a UV-visible spectrophotometer (Optizen POP) at wavelength from 250 to 800 nm. The concentration of methylene blue in the solution was determined as a function of irradiation time from the absorbance change at a wavelength of 664 nm.

For the hydrogen evolution, the photocatalyst powder 50 mg as-prepared samples were dispersed by magnetic stirrer, in 150 mL aqueous solution containing 0.1 mol L^{-1} Na_2S and 0.04 mol L^{-1} Na_2SO_3 and 20 % methanol as a sacrificial reagent. UV light source having 356 nm in wavelength was used at a distance of 20 cm from the glass reactor. After 20 h, the amount of hydrogen gas evolved was detected by Minimax (X13010683) XP H_2 sensor.

RESULTS AND DISCUSSION

Fig. 1 shows the XRD patterns of (a) JCPDS 29-0351 data of $CaMoO_4$ and the synthesized (b) 5 wt % TiO_2 coated $CaLa_2(MoO_4)_4$, (c) 10 wt % TiO_2 coated $CaLa_2(MoO_4)_4$, (d) 15 wt % TiO_2 coated $CaLa_2(MoO_4)_4$ nano core-shells. The crystal structure of $CaLa_2(MoO_4)_4$ is not present in the JCPDS data. However, the XRD peaks in Fig. 1 are similar to the phase based ones on the tetragonal $CaMoO_4$ with a scheelite-type structure of space group $I4_1/a$. Secondary phases were detected at 25.5°, 46.5°, 52.5° in Fig. 1(b), (c) and (d). The foreign reflexes marked with an asterisk in Fig. 1(b), (c) and (d) were identified to the TiO_2 as anatase phases.

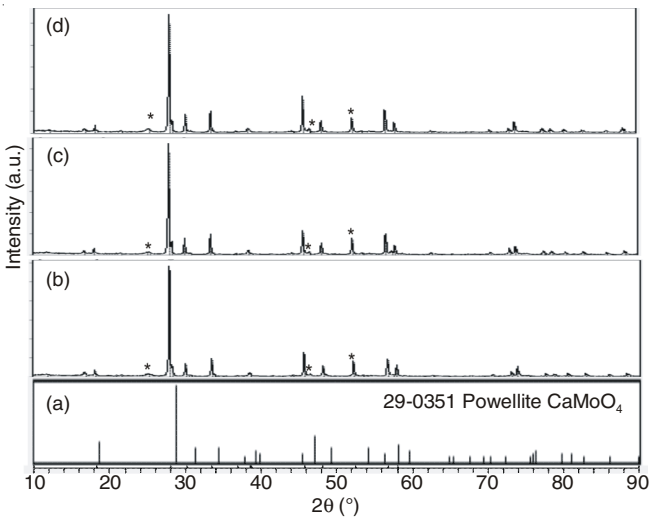

Fig. 1. X-ray diffraction patterns of (a) JCPDS 29-0351data of $CaMoO_4$ and the synthesized (b) 5 wt % TiO_2 coated $CaLa_2(MoO_4)_4$, (c) 10 wt % TiO_2 coated $CaLa_2(MoO_4)_4$, (d) 15 wt % TiO_2 coated $CaLa_2(MoO_4)_4$ nano core-shells

Fig. 2 shows TEM microscopy images of the (a) 5 wt % TiO_2 coated $CaLa_2(MoO_4)_4$, (b) 10 wt % TiO_2 coated $CaLa_2(MoO_4)_4$, (c) 15 wt % TiO_2 coated $CaLa_2(MoO_4)_4$ nano core-shells. The morphological features are almost similar showing the outer phases of TiO_2 and black core phases of $CaLa_2(MoO_4)_4$. The agglomerates are observed in the case of (a) 5 wt % TiO_2 coated $CaLa_2(MoO_4)_4$ and (c) 15 wt % TiO_2 coated $CaLa_2(MoO_4)_4$ nano core-shells. The core-shell structures are clearly observed in (b) 10 wt % TiO_2 coated $CaLa_2(MoO_4)_4$ and (c) 15 wt % TiO_2 coated $CaLa_2(MoO_4)_4$ with diameters of 10-20 nm. TiO_2 coated $CaLa_2(MoO_4)_4$ nano core-shells were successfully synthesized using two-step procedures of the microwave sol-gel method for the core-cell of $CaLa_2(MoO_4)_4$ and ultrasonic method for the outer phase of TiO_2.

The characteristic UV/visible absorption intensity of methylene blue at 664 nm decreased on increasing the time interval [23] for TiO_2 coated updoped $CaLa_2(MoO_4)_4$ in Fig. 3 and TiO_2 coated doped $CaLa_{1.7}(MoO_4)_4$:$Er_{0.1}Yb_{0.2}$ in Fig. 4. The degradation efficiencies of the 5 wt % TiO_2 coated $CaLa_2(MoO_4)_4$,

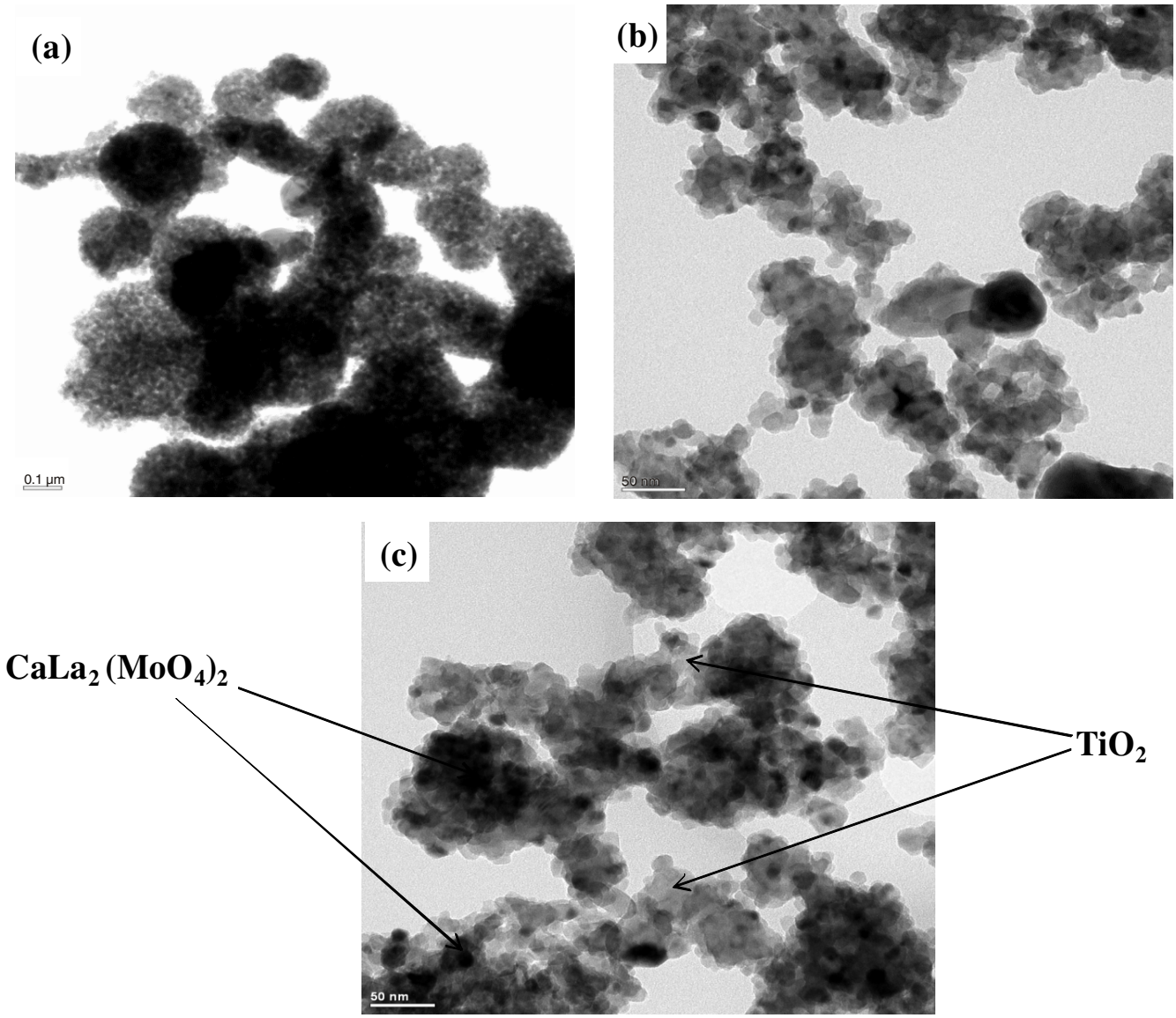

Fig. 2. Transmission electron microscopy images of the (a) 5 wt % TiO_2 coated $CaLa_2(MoO_4)_4$, (b) 10 wt % TiO_2 coated $CaLa_2(MoO_4)_4$, (c) 15 wt % TiO_2 coated $CaLa_2(MoO_4)_4$ nano core-shells

10 wt % TiO_2 coated $CaLa_2(MoO_4)_4$ and 15 wt % TiO_2 coated $CaLa_2(MoO_4)_4$ nano core-shells are shown in Fig. 3(a-c). The controlled experiment for the degradation of methylene blue over as-prepared samples was also carried out. The results are depicted in Fig. 3(d). From the results of Fig. 3(d) it is clear that the degradation efficiency increases with the introduction of TiO_2 in the samples [20]. The overall catalytic efficiency of TiO_2 coated undoped $CaLa_2(MoO_4)_4$ is in the order of 10 wt % > 15 wt % > 5 wt %. The degradation efficiencies of the 5 wt % TiO_2 coated $CaLa_{1.7}(MoO_4)_4$: $Er_{0.1}Yb_{0.2}$, 10 wt % TiO_2 coated $CaLa_{1.7}(MoO_4)_4$:$Er_{0.1}Yb_{0.2}$ and 15 wt % TiO_2 coated $CaLa_{1.7}(MoO_4)_4$: $Er_{0.1}Yb_{0.2}$ nano core-shells are shown in Fig. 4(a-c). The overall catalytic efficiency of TiO_2 coated doped $CaLa_{1.7}(MoO_4)_4$:$Er_{0.1}Yb_{0.2}$ is also same as the case of the TiO_2 coated undoped $CaLa_2(MoO_4)_4$ in the order of 10 wt % > 15 wt % > 5 wt %. These results clearly show that most of the methylene blue was degraded by the 10 wt % catalyst over the period of 150 min, concluding that the 10 % catalyst exhibits the highest synergetic effect between TiO_2 and the $CaLa_2(MoO_4)_4$ and $CaLa_{1.7}(MoO_4)_4$:$Er_{0.1}Yb_{0.2}$. Light irradiation produces electrons (e^-) in the conduction band (CB) and holes (h^+) in the valence band (VB) of TiO_2 in the nanocomposite. Meanwhile, the generated electron was transferred to the conduction band of $CaLa_2(MoO_4)_4$ and $CaLa_{1.7}(MoO_4)_4$:$Er_{0.1}Yb_{0.2}$, thereby increasing the number of electrons as well as the rate of electron-induced redox reactions. The $CaLa_2(MoO_4)_4$ and $CaLa_{1.7}(MoO_4)_4$:$Er_{0.1}Yb_{0.2}$ supported by TiO_2 system shows enhanced catalytic activity due to high charge separation induced by the synergetic effects of $CaLa_2(MoO_4)_4$, $CaLa_{1.7}(MoO_4)_4$:$Er_{0.1}Yb_{0.2}$ and TiO_2. This enhancement of catalytic effect is attributed to the incorporation of TiO_2 in the $CaLa_2(MoO_4)_4$ and $CaLa_{1.7}(MoO_4)_4$:$Er_{0.1}Yb_{0.2}$ system.

Fig. 5 shows apparent first order kinetics of degradation of methylene blue under visible light for (A) TiO_2 coated undoped $CaLa_2(MoO_4)_4$; (a) 5 wt % TiO_2 coated $CaLa_2(MoO_4)_4$, (b) 10 wt % TiO_2 coated $CaLa_2(MoO_4)_4$ and (c) 15 wt % TiO_2 coated $CaLa_2(MoO_4)_4$ and (B) TiO_2 coated doped $CaLa_{1.7}(MoO_4)_4$: $Er_{0.1}Yb_{0.2}$; (a) 5 wt % TiO_2 coated $CaLa_{1.7}(MoO_4)_4$:$Er_{0.1}Yb_{0.2}$, (b) 10 wt % TiO_2 coated $CaLa_{1.7}(MoO_4)_4$:$Er_{0.1}Yb_{0.2}$, (c) 15 wt % TiO_2 coated $CaLa_{1.7}(MoO_4)_4$:$Er_{0.1}Yb_{0.2}$ nano core-shells. The kinetics for different photocatalysts can be expressed by the Langmuire-Hinshelwood model [24]. The photocatalytic degradation of methylene blue containing different photocatalysts obeyed pseudo-first order kinetics with respect to the concentration of methylene blue.

$$-dC/dt = K_{app}c \quad (1)$$

Integrating eqn. 1 (with the restriction $C = C_0$ at $t = 0$ with C_0 being the initial concentration in the bulk solution after

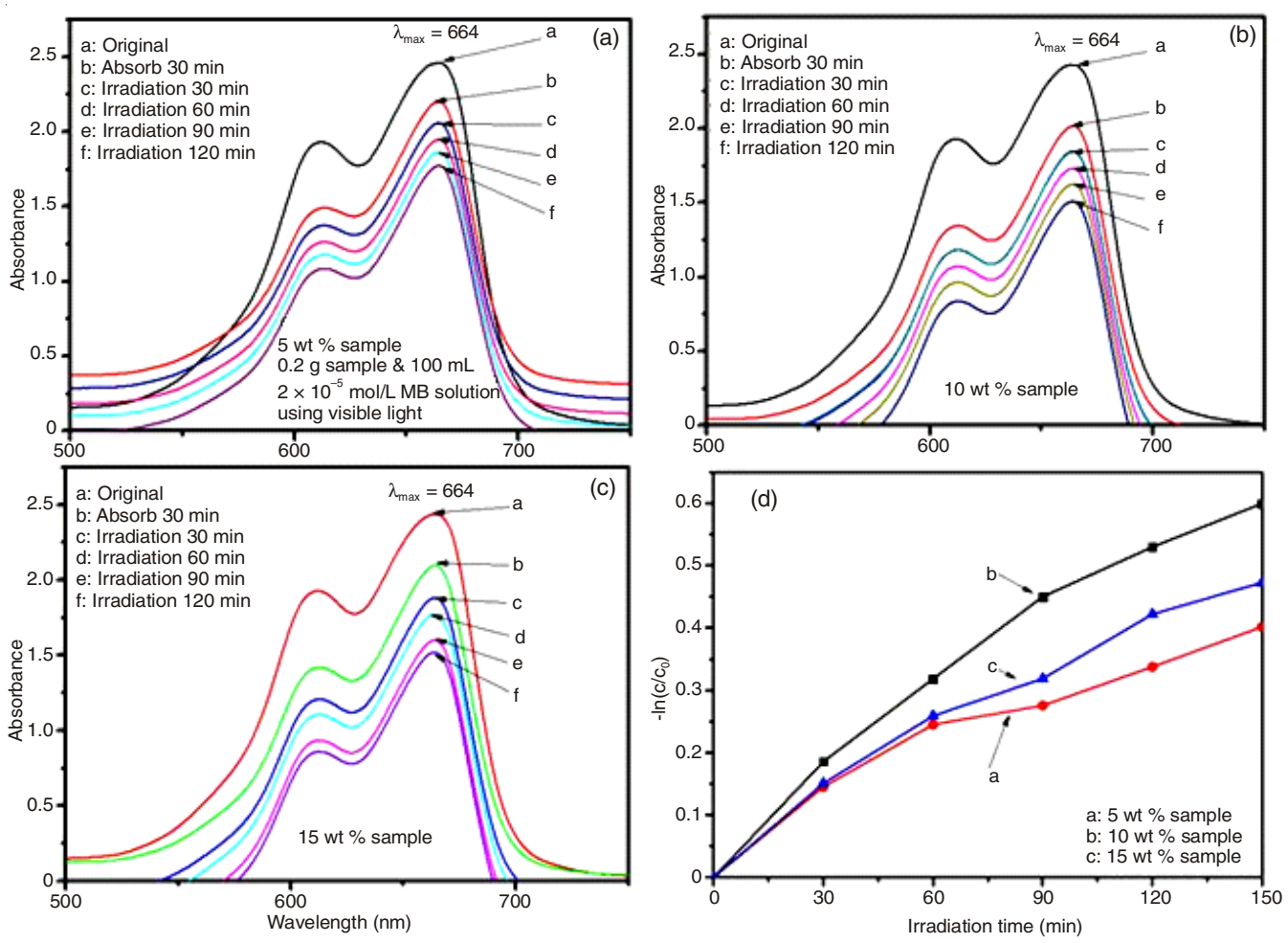

Fig. 3. Photo degradation of methylene blue solution under visible light for TiO_2 coated undoped $CaLa_2(MoO_4)_4$; (a) 5 wt % TiO_2 coated $CaLa_2(MoO_4)_4$, (b) 10 wt % TiO_2 coated $CaLa_2(MoO_4)_4$, (c) 15 wt % TiO_2 coated $CaLa_2(MoO_4)_4$ nano core-shells and (d) apparent first order kinetics methylene blue degradation

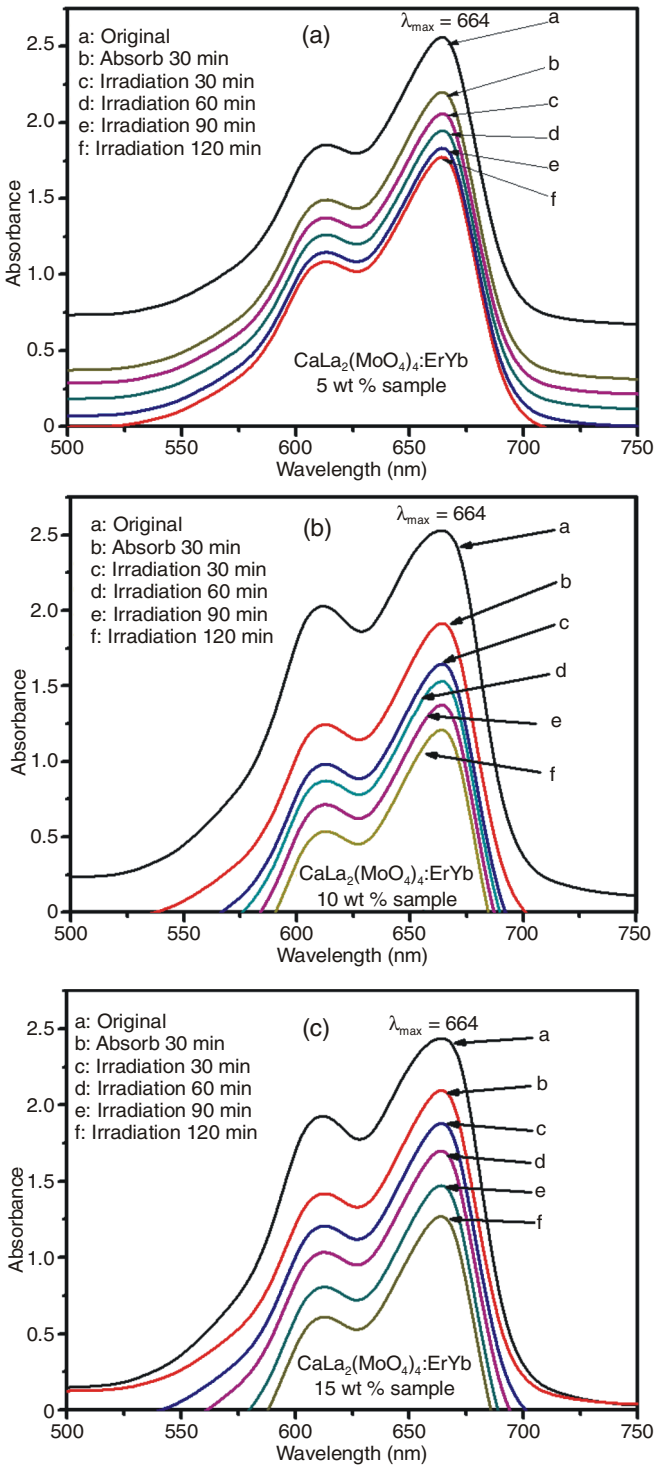

Fig. 4. Photo degradation of methylene blue solution under visible light for TiO_2 coated doped $CaLa_{1.7}(MoO_4)_4:Er_{0.1}Yb_{0.2}$; (a) 5 wt % TiO_2 coated $CaLa_{1.7}(MoO_4)_4:Er_{0.1}Yb_{0.2}$, (b) 10 wt % TiO_2 coated $CaLa_{1.7}(MoO_4)_4:Er_{0.1}Yb_{0.2}$, (c) 15 wt % TiO_2 coated $CaLa_{1.7}(MoO_4)_4:Er_{0.1}Yb_{0.2}$ nano core-shells

dark adsorption and the reaction time) will lead to the following relation:

$$-\ln (C_t/C_0)=K_{app}t \quad (2)$$

where C_t and C_0 are the reactant concentrations at times t and t = 0, respectively. Also, K_{app} and t are the apparent reaction rate constant and time, respectively. According to this equation, a plot of $-\ln (C_t/C_0)$ *versus* t will yield a slope of K_{app}. The insert indicates the degradation rate constants of methylene blue under visible light irradiations of (a)-(c) in Fig. 5(a) and 5(b). The degradation rate constants of methylene blue under visible light irradiation in Fig. 5(a) are 1.69×10^{-3} min^{-1} for (a) 5 wt % TiO_2 coated $CaLa_2(MoO_4)_4$ and 1.99×10^{-3} min^{-1} for (c) 15 wt % TiO_2 coated $CaLa_2(MoO_4)_4$. The methylene blue degradation rate const under visible light irradiation for (b) 10 wt % TiO_2 coated $CaLa_2(MoO_4)_4$ results in 2.24×10^{-3} min^{-1}, which provides much higher value than those for (a) 5 wt % TiO_2 coated $CaLa_2(MoO_4)_4$ and (c) 15 wt % TiO_2 coated $CaLa_2(MoO_4)_4$. The methylene blue degradation rate constants under visible light irradiation in Fig. 5(b) are 1.66×10^{-3} min^{-1} for (a) 5 wt % TiO_2 coated $CaLa_{1.7}(MoO_4)_4:Er_{0.1}Yb_{0.2}$ and 1.69×10^{-3} min^{-1} for (c) 15 wt % TiO_2 coated $CaLa_{1.7}(MoO_4)_4:Er_{0.1}Yb_{0.2}$. The methylene blue degradation rate const under visible light irradiation for (b) 10 wt % TiO_2 coated $CaLa_{1.7}(MoO_4)_4:Er_{0.1}Yb_{0.2}$ results in 3.48×10^{-3} min^{-1}, which provides much higher value than those for (a) 5 wt % TiO_2 coated $CaLa_{1.7}(MoO_4)_4:Er_{0.1}Yb_{0.2}$ and (c) 15 wt % TiO_2 coated $CaLa_{1.7}(MoO_4)_4:Er_{0.1}Yb_{0.2}$. The methylene blue degradation rate constant of 10 wt % TiO_2 coated doped $CaLa_{1.7}(MoO_4)_4:Er_{0.1}Yb_{0.2}$ is higher than that of the 10 wt % TiO_2 coated undoped $CaLa_2(MoO_4)_4$.

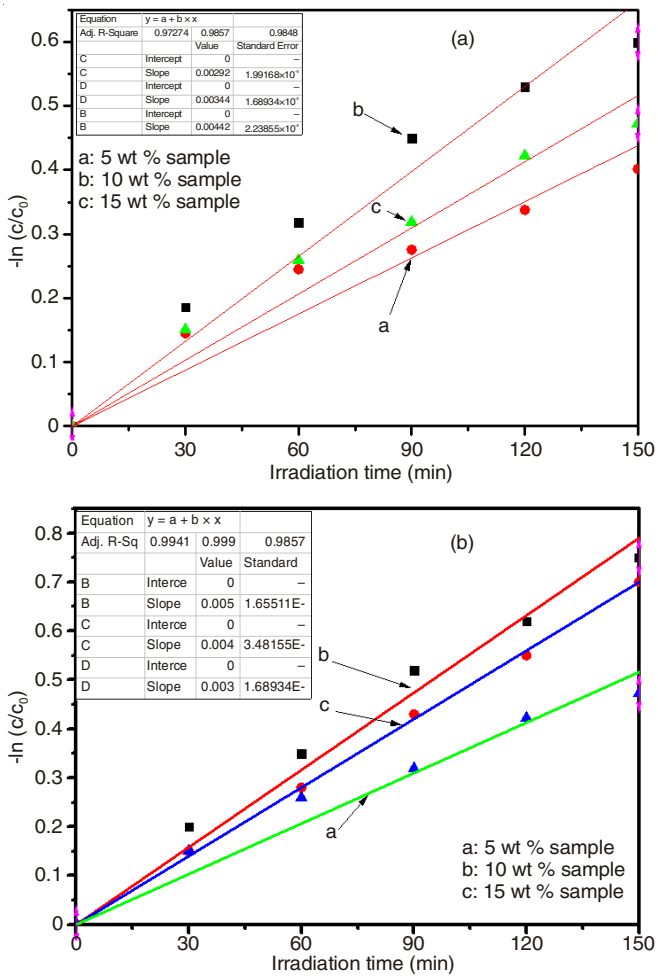

Fig. 5. Apparent first order kinetics of methylene blue degradation under visible light; (a) TiO_2 coated undoped $CaLa_2(MoO_4)_4$ and (b) TiO_2 coated doped $CaLa_{1.7}(MoO_4)_4:Er_{0.1}Yb_{0.2}$ nano core-shells

Fig. 6 shows photocatalytic H_2 evolution of (a) 5 wt % sample, (b) 10 wt % sample, (c) 15 wt % sample for the TiO_2

coated $CaLa_{1.5}(MoO_4)_4$:$Er_{0.05}Yb_{0.45}$ and (d) P-25 dispersed in 100mL aqueous solution containing Na_2S/Na_2SO_3 as a sacrificial reagent. The TiO_2 nanoparticles on the $CaLa_{1.5}(MoO_4)_4$:$Er_{0.05}Yb_{0.45}$ surface act as H_2 evolution centers, as decorated by the ultrasonicated method. A 356 nm light source was adjusted so that the maximum area of the sealed container would be exposed. Quantum yield (QY) was observed using the equation [25].

$$n_p = t \times S \times Q \quad (3)$$

$$QY\ (\%) = n_H/n_p \times 100 \quad (4)$$

where, n_p is the amount of incident photons, t is irradiation time, s is irradiation area in m^2 and Q is photon flux of the incident light in eqn. 3. The quantum yield was calculated from the ratio of the number of reacted electrons during hydrogen evolution to the number of incident photons according to eqn. 4, where n_H is the amount of photogenerated H_2 [21] for the TiO_2 coated $CaLa_{1.5}(MoO_4)_4$:$Er_{0.05}Yb_{0.45}$ samples and P-25 are shown in Figs. 6 and 7, respectively. The quantum yields of individual 10 wt % sample were the best with 6.19 %, using Na_2S/Na_2SO_3 as the reagent. In contrast, H_2 evolution and quantum yield for P-25 were smaller than those of the TiO_2 coated $CaLa_{1.5}(MoO_4)_4$:$Er_{0.05}Yb_{0.45}$ samples under the same conditions. The decrease in H_2 evolution and corresponding quantum yield efficiency may have been attributed to the fast recombination rate of the excited electrons and holes pair in TiO_2 [26]. These results highlight the importance of TiO_2 coated $CaLa_{1.5}(MoO_4)_4$:$Er_{0.05}Yb_{0.45}$, which is absent in P-25.

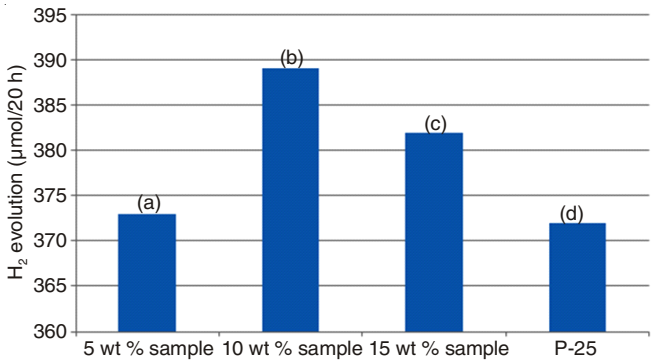

Fig. 6. Photocatalytic H_2 evolution of (a) 5 wt % sample, (b)10 wt % sample, (c) 15 wt % sample for the TiO_2 coated $CaLa_{1.5}(MoO_4)_4$:$Er_{0.05}Yb_{0.45}$ and (d) P-25 using Na_2S/Na_2SO_3 as the sacrificial reagent

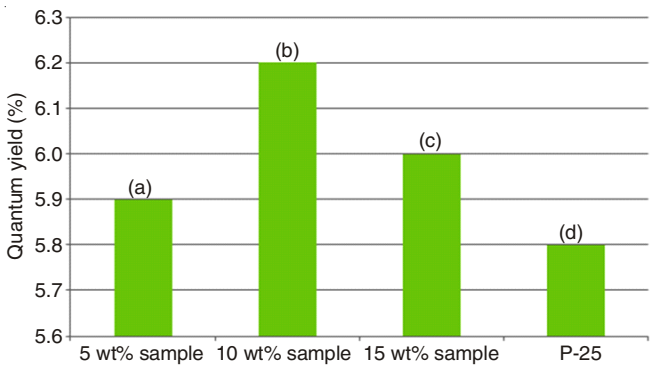

Fig. 7. Quantum yields for hydrogen evolution by (a) 5 wt % sample, (b) 10 wt % sample, (c) 15 wt % sample for the TiO_2 coated $CaLa_{1.5}(MoO_4)_4$:$Er_{0.05}Yb_{0.45}$ and (d) P-25 with the Na_2S/Na_2SO_3 aqueous solution

The sacrificial reagent provided electrons to consume the photogenerated holes and TiO_2 acted as a reaction center to produce H_2 from water.

Cyclic photocatalytic hydrogen evolution experiments were carried out to further demonstrate the photostability and cyclic performance of the 10 wt % TiO_2 coated $CaLa_{1.5}(MoO_4)_4$:$Er_{0.05}Yb_{0.45}$. As shown in Fig. 8, the photocatalysts exhibited a minor loss of photocatalytic activity for hydrogen evolution under the same conditions after four runs, indicating the photocatalytic stability of our nanocomposite [27]. The reused catalyst did not show any noticeable change in quantum yields efficiency, which emphasizes the excellent chemical stability of the catalysts and their benefit in practical applications.

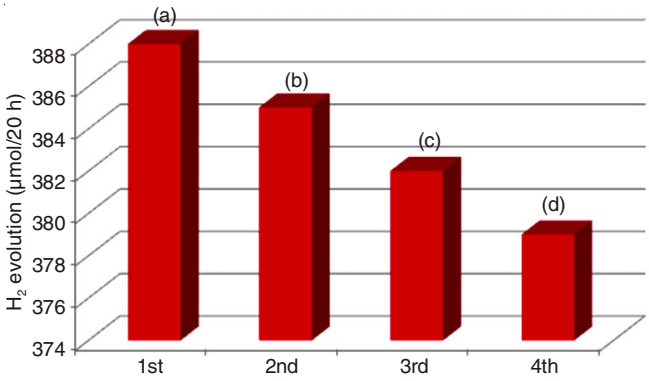

Fig. 8. Cyclic test of (a) 1st, (b) 2nd, (c) 3rd and (d) 4th for the 10 wt % TiO_2 coated $CaLa_{1.5}(MoO_4)_4$:$Er_{0.05}Yb_{0.45}$ sample using Na_2S/Na_2SO_3 as the sacrificial reagent under UV light irradiation

Fig. 9 shows upconversion photoluminescence emission spectra of (a) $CaLa_2(MoO_4)_4$, (b) $CaLa_{1.8}(MoO_4)_4$:$Er_{0.2}$, (c) $CaLa_{1.7}(MoO_4)_4$:$Er_{0.1}Yb_{0.2}$ and (d) $CaLa_{1.5}(MoO_4)_4$:$Er_{0.05}Yb_{0.45}$ particles excited under 980 nm at room temperature. The upconversion intensity of (a) $CaLa_2(MoO_4)_4$ and (b) $CaLa_{1.8}(MoO_4)_4$:$Er_{0.2}$ were not detected. The UC (c) $CaLa_{1.7}(MoO_4)_4$:$Er_{0.1}Yb_{0.2}$ and (d) $CaLa_{1.5}(MoO_4)_4$:$Er_{0.05}Yb_{0.45}$ particles exhibited a strong 525 nm emission band, a weak 550 nm emission band in the green region and a very weak 655 nm emission band in the red region. The strong 525 nm emission band and the weak 550 nm emission band in the green region correspond to the $^2H_{11/2} \rightarrow {}^4I_{15/2}$ and $^4S_{3/2} \rightarrow {}^4I_{15/2}$ transitions, respectively, while the very weak emission 655 nm band in the red region corresponds to the $^4F_{9/2} \rightarrow {}^4I_{15/2}$ transition. The upconversion intensity of (d) $CaLa_{1.5}(MoO_4)_4$:$Er_{0.05}Yb_{0.45}$ is higher than that of (c) $CaLa_{1.7}(MoO_4)_4$:$Er_{0.1}Yb_{0.2}$.

Fig. 10 shows CIE chromaticity diagram showing the colour coordinates of the $CaLa_{2-x}MoO_4$:Er^{3+}/Yb^{3+} phosphors. The inset shows the emissions for the sample synthesized (a) $CaLa_2(MoO_4)_4$, (b) $CaLa_{1.8}(MoO_4)_4$:$Er_{0.2}$, (c) $CaLa_{1.7}(MoO_4)_4$:$Er_{0.1}Yb_{0.2}$ and (d) $CaLa_{1.5}(MoO_4)_4$:$Er_{0.05}Yb_{0.45}$ particles. The colour coordinates of the samples have a good match with the standard point of equal energy. The yellowish green emissions can be found for the samples of (c) $CaLa_{1.7}(MoO_4)_4$:$Er_{0.1}Yb_{0.2}$ and (d) $CaLa_{1.5}(MoO_4)_4$:$Er_{0.05}Yb_{0.45}$ particles. This result provides to achieve the attractive yellowish green upconversion emissions under considering the potentially active components in new optoelectronic devices and luminescent devices.

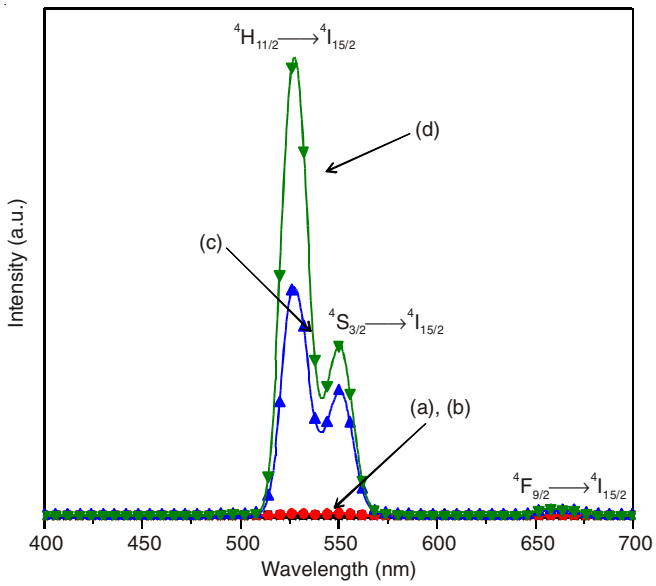

Fig. 9. Upconversion photoluminescence emission spectra of (a) $CaLa_2(MoO_4)_4$, (b) $CaLa_{1.8}(MoO_4)_4:Er_{0.2}$, (c) $CaLa_{1.7}(MoO_4)_4:Er_{0.1}Yb_{0.2}$ and (d) $CaLa_{1.5}(MoO_4)_4:Er_{0.05}Yb_{0.45}$ particles excited under 980 nm at room temperature

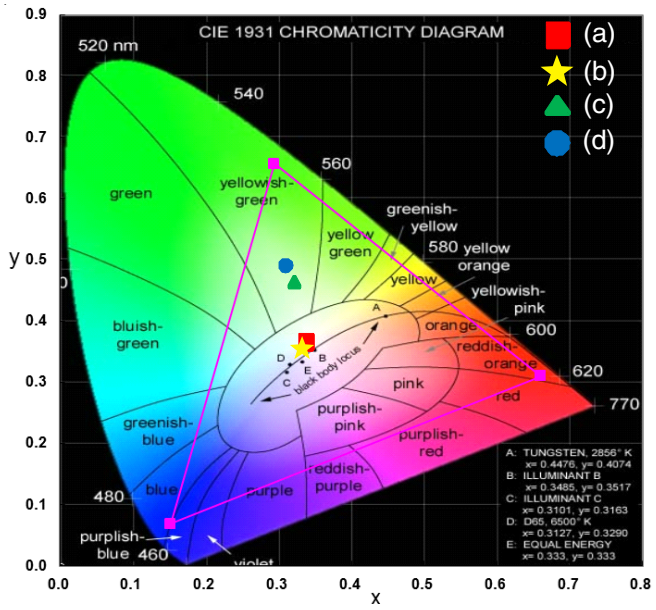

Fig. 10. CIE chromaticity diagram showing the colour coordinates of the $CaLa_{2-x}(MoO_4)_4:Er^{3+}/Yb^{3+}$ phosphors. The inset shows the emissions for the sample synthesized (a) $CaLa_2(MoO_4)_4$, (b) $CaLa_{1.8}(MoO_4)_4:Er_{0.2}$, (c) $CaLa_{1.7}(MoO_4)_4:Er_{0.1}Yb_{0.2}$ and (d) $CaLa_{1.5}(MoO_4)_4:Er_{0.05}Yb_{0.45}$ particles

Conclusion

Titanium(IV) dioxide coated undoped $CaLa_2(MoO_4)_4$ and doped $CaLa_{2-x}(MoO_4)_4$:Er/Yb nano core-shells were successfully synthesized using two-step procedures of the microwave sol-gel and ultrasonic methods. Well-crystallized nano core-shells showed a fine and homogeneous morphology with particle sizes of 10-20 nm. The degradation efficiency of methylene blue for the samples for TiO_2 coated undoped $CaLa_2(MoO_4)_4$ and doped $CaLa_{1.7}(MoO_4)_4:Er_{0.1}Yb_{0.2}$ nano core-shells under visible light resulted in the order as 10 wt % > 15 wt % > 5 wt %. The degradation rate constant of methylene blue 10 wt % TiO_2 coated doped $CaLa_{1.7}(MoO_4)_4:Er_{0.1}Yb_{0.2}$ is higher than that of the 10 wt % TiO_2 coated undoped $CaLa_2(MoO_4)_4$. Quantum yield of the nano core-shells for the hydrogen evolution provided the best result for 10 wt % of TiO_2 coated $CaLa_{1.5}(MoO_4)_4$: $Er_{0.05}Yb_{0.45}$ with 6.19 %, using Na_2S/Na_2SO_3 as the reagent. Under excitation at 980 nm, the UC $CaLa_{1.7}(MoO_4)_4:Er_{0.1}Yb_{0.2}$ and $CaLa_{1.5}(MoO_4)_4:Er_{0.05}Yb_{0.45}$ particles exhibited a strong 525 nm emission band and a weak 550 nm emission band in the green region. The CIE chromaticity diagram of the colour coordinates showed a good match with yellowish green emissions for the samples of $CaLa_{1.7}(MoO_4)_4:Er_{0.1}Yb_{0.2}$ and $CaLa_{1.5}(MoO_4)_4:Er_{0.05}Yb_{0.45}$ particles.

ACKNOWLEDGEMENTS

This research was supported by the Basic Science Research Program through National Research Foundation of Korea (NRF) funded by the Ministry of Education (2015-058813).

REFERENCES

1. K. Ullah, Z. Lei, S. Ye, A. Ali and W.C. Oh, *RSC Adv.*, **5**, 18841 (2015).
2. L. Lin, H.Y. Wang, H.G. Luo and P. Xu, *J. Photochem. Photobiol. Chem.*, **307–308**, 88 (2015).
3. K. Ullah, L. Zhu, Z.-D. Meng, S. Ye, Q. Sun and W.C. Oh, *Chem. Eng. J.*, **231**, 76 (2013).
4. J. Zhang, W.C. Wu, S. Yan, G. Chu, S.L. Zhao, X. Wang and C. Li, *Appl. Surf. Sci.*, **344**, 249 (2015).
5. L. Zhu, S.-B. Jo, S. Ye, K. Ullah, Z.-D. Meng and W.-C. Oh, *J. Ind. Eng. Chem.*, **22**, 264 (2015).
6. Z. Lei and W.C. Oh, *J. Mutifunct. Mater. Photosci.*, **5**, 153 (2014).
7. M.V. DaCosta, S. Doughan, Y. Han and U.J. Krull, *Anal. Chim. Acta*, **832**, 1 (2014).
8. M. Lin, Y. Zhao, S.Q. Wang, M. Liu, Z.F. Duan, Y.M. Chen, F. Li, F. Xu and T.J. Lu, *Biotechnol. Adv.*, **30**, 1551 (2012).
9. M. Wang, G. Abbineni, A. Clevenger, C. Mao and S. Xu, *Nanomedicine*, **7**, 710 (2011).
10. J. Sun, W. Zhang, W. Zhang and H. Du, *Mater. Res. Bull.*, **47**, 786 (2012).
11. S. Huang, Z. Lou, Z. Qi, N. Zhu and H. Yuan, *Appl. Catal. B*, **168-169**, 313 (2015).
12. J. Zhang, H. Shen, W. Guo, S. Wang, C. Zhu, F. Xue, J. Hou, H. Su and Z. Yuan, *J. Power Sources*, **226**, 47 (2013).
13. S. Huang, Z. Lou, N. Zhu and H. Yuan, *Catal. Commun.*, **61**, 6 (2015).
14. W. Wang, M. Ding, C. Lu, Y. Ni and Z. Xu, *Appl. Catal. B*, **144**, 379 (2014).
15. Q.-L. Ye, X. Yang, C. Li and Z. Li, *Mater. Lett.*, **106**, 238 (2013).
16. T. Ji, F. Yang, H. Du, H. Guo and J. Yang, *J. Rare Earths*, **28**, 529 (2010).
17. D.-X. Xu, Z.-W. Lian, M.-L. Fu, B. Yuan, J.-W. Shi and H.-J. Cui, *Appl. Catal. B*, **142-143**, 377 (2013).
18. A.A. Ansari and M. Alam, *J. Lumin.*, **157**, 257 (2015).
19. J. Sun, X. Gao, D. He, J. Chen, X. Meng, Q. Zhang, L. Shen and H. Jiao, *Particulogy*, **11**, 776 (2013).
20. L.M. Pastrana-Martínez, S. Morales-Torres, V. Likodimos, J.L. Figueiredo, J.L. Faria, P. Falaras and A.M.T. Silva, *Appl. Catal. B*, **123–124**, 241 (2012).
21. L. Li, B. Cheng, Y. Wang and J. Yu, *J. Colloid Interface Sci.*, **449**, 115 (2015).
22. W. Bu, Y. Xu, N. Zhang, H. Chen, Z. Hua and J. Shi, *Langmuir*, **23**, 9002 (2007).
23. K. Ullah, S. Ye, L. Zhu, Z.-D. Meng, S. Sarkar and W.-C. Oh, *Mater. Sci. Eng. B*, **180**, 20 (2014).
24. X. Li, W. Cai, J. An, S. Kim, J. Nah, D. Yang, R. Piner, A. Velamakanni, I. Jung, E. Tutuc, S.K. Banerjee, L. Colombo and R.S. Ruoff, *Science*, **324**, 1312 (2009).
25. S. Ye, K. Ullah, L. Zhu, A. Ali, W.K. Jang and W.C. Oh, *Solid State Sci.*, **46**, 84 (2015). (In press).
26. W. Ho, Z. Zhang, M. Xu, X. Zhang, X. Wang and Y. Huang, *Appl. Catal. B*, **179**, 106 (2015).
27. R. Wess, F. Nores-Pondal, M. Laborde and P. Giunta, *Chem. Eng. Sci.*, **134**, 86 (2015).